17th World Conference on Earthquake Engineering, 17WCEE

Sendai, Japan - September 13th to 18th 2020

EXPERIMENTAL OBSERVATION OF SEISMIC PERFORMANCE FOR RC BRIDGE COLUMNS WITH HIGH STRENGTH REINFORCEMENT

D.H. Lee[(1)], J.-H. Lee[(2)]

[(1)] *Professor, Department. of Civil, Environmental and Railroad Engineering, PaiChai University, Daejeon 35345, South Korea, dohlee@pcu.ac.kr*

[(2)] *Professor, Department of Civil Engineering, Yeungnam University, Gyeongsan 38541, South Korea, jhl79@ynu.ac.kr*

Abstract

An experiment has been conducted for the seismic performance evaluation on reinforced concrete bridge columns employing both normal and high strength reinforcement of SD400 and SD700, respectively. For this purpose, a total of 12 specimens, i.e., 6 circular columns and 6 square columns have been designed and tested under repeated lateral deformation reversals. In the design of such columns, various design parameters have been included, such as types of cross section, yield strength of both longitudinal and lateral reinforcements, diameter and ratio of longitudinal reinforcement, vertical spacing and volumetric ratio of lateral reinforcement. Lateral force-displacement hysteretic response reveals that experimentally obtained lateral forces are in general well above the code-specified lateral strength in overall displacement range. A difference between the two lateral forces is more marginal in specimens with SD700 of longitudinal reinforcement than specimens with SD400 of longitudinal reinforcement, particularly for circular columns. Although both specimens show stable response, the latter exhibits somewhat more ductile behavior than the former. Maximum lateral strength indicates that experimental results are in general higher than code-specified theoretical predictions. The difference is more pronounced for specimens with SD700 of longitudinal reinforcement, as expected. In addition, deformation capacity is also investigated using displacement ductility and cumulative energy. Whereas experimental ductility values are in general greater than code-specified values, margin of safety is reduced as yield strength and ratio of longitudinal reinforcement increase. This is supported by the observation of cumulative energy. The cumulative energy also decreases as yield strength of longitudinal reinforcement becomes higher. In all, use of high yield strength reinforcement in reinfored concrete bridge columns has apparently a favorable effect on the maximum strength throughout overall displacement range. However, the current evaluation on deformation capacity indicates less marginal for specimens with high yield strength reinforcement. It is thus concluded that further experiment is required to investigate the deformation capacity of the columns with high yield strength reinforcement.

Keywords: RC column; high strength reinforcement; load-carrying capacity; displacement ductility; energy dissipation

1. Introduction

Reinforced concrete bridge columns generally are large in size and thus require a large amount of reinforcement. Subsequently, use of high yield strength steel reinforcement in these members may lead to a wider spacing of reinforcement arrangement and a potential reduction in total amount of reinforcement. This may also result in an easy concrete placing and thus an improved constructability and cost-effective.
Study on the applicability of high strength reinforcement has been initiated from the development of Martensitic Microcomposite Formable Steel (referred to as MMFX) reinforcement having 690 MPa and 830 MPa of yield strength reinforcement. Ansley [1] conducted an experimental work on reinforced concrete beams with MMFX reinforcement instead of using 420 MPa of reinforcement. Watanabe and Nishiyama [2] performed cyclic test on reinforced concrete bridge columns subjected to simulated earthquake loading. Based on the test, they proposed a combination scheme using both high and normal yield strength of longitudinal reinforcements. Hassan et al. [3], Mast et al. [4] and Sumpter et al. [5] amongst many others also carried out reinforced concrete beam tests using MMFX high strength reinforcements. Some of research work have been carried out in South Korea for the application of high strength reinforcements on reinforced concrete members. A research work on ultra-bar was carried out for the applicability of 600 MPa and 500 MPa of steels on longitudinal and shear reinforcements, respectively [6, 7, 8]. In addition, work on the applicability of 600 MPa and 700 MPa of steel was also performed for reinforced concrete members [9, 10, 11]. However, performance evaluation on reinforced concrete columns with more than 600 MPa of high strength reinforcement has neither been conducted qualitatively nor quantitatively. This is mainly due to a limitation on code-specified yield strength.

Specified yield strength of reinforcement for reinforced concrete columns is varied between design codes. ACI 318-14 [12] specifies 420 MPa and 550 MPa of yield strength for flexure and axial reinforcement of special seismic systems and other, respectively. As for lateral reinforcement, ACI 318-14 [12] specifies 700 MPa and 550 MPa of yield strength for spirals or special seismic systems and other, respectively. Eurocode 2 [13] specifies the yield strength of 600 MPa for all reinforcements. In South Korea, two codes can be applied for the design of reinforced concrete bridge columns. Korea Road and Transportation Association design code for highway bridges-limit state design (referred to as KRTA [14] hereafter) specifies yield strength of 600 MPa for all reinforcements as identical to Eurocode 2 [13]. However, the KRTA [14] limits yield strength to 500 MPa for both axial and lateral reinforcements in case of seismic design. In addition, Korea Concrete Institute model code (referred to as KCI [15] hereafter) also specifies 600 MPa of yield strength for flexure and axial reinforcement. KCI [15] however limits yield strength to 500 MPa and 700 MPa for shear and lateral reinforcement, respectively. It is noteworthy that Korean Standard D 3504 [16] steel bars for concrete reinforcement has regulated SD700 (700 MPa of nominal yield strength) for concrete reinforcement. Nonetheless, SD700 reinforcement has not been used in everyday practice since the design codes limit the yield strength not more than 600 MPa.

In view of the above, experimental study was conducted for the applicability of high yield strength of reinforcements on reinforced concrete columns. For this purpose, reinforced concrete circular and square columns employing SD700 reinforcements were tested under simulated cyclic loading. In addition, those members with SD400 (400 MPa of nominal yield strength) reinforcements were also tested for comparison purpose. Detailed description on the experimental work is addressed hereafter.

2. Experiment

2.1 Bridge column specimens

To investigate the applicability of SD700 high strength reinforcing steel bars on both longitudinal and lateral reinforcements in columns, a total of 12, i.e., 6 circular and 6 square cross sections, column specimens were designed and fabricated. Circular column specimens had a cross sectional diameter of 400 mm and square column specimens had a cross section of 350 × 350 mm. Cross section arrangement is to set longitudinal reinforcement and applied axial force ratio as almost identical in both column specimens.

Height from the surface of column foundation to the lateral loading point was 1,400 mm in all column specimens, leading the aspect ratios of 3.5 and 4 for circular and square column specimens, respectively. Accordingly, flexural behavior is expected dominantly in both columns. Applied axial forces were 377 kN and 368 kN for circular and square columns, respectively, being a constant axial force ratio of 12.5 % in both column specimens. Compressive strength of concrete was 24 MPa at the time of test, and longitudinal reinforcement ratio, yield strength of reinforcements and vertical spacing of lateral reinforcement were selected as primary design variables in the present test. Material properties and design details of test variables are summarized in Table 1, and dimensions and cross section details are illustrated in Fig. 1.

Table 1 – Design parameters of column specimens

Specimen	Cross section	Compressive concrete strength (MPa)	Longitudinal reinforcement		Transverse reinforcement			Aspect ratio	Applied axial force ratio $\frac{P}{f_{ck}A_g}$
			Ratio ρ_l (%)	Yield strength (MPa)	Vertical spacing (mm)	Ratio ρ_s (%)	Yield strength (MPa)		
C16-80-77	Circular	24	1.27	707	80	1.1	750	3.5	0.125
C16-80-74				707	80	1.1	495		
C16-80-47				516	80	1.1	750		
C16-60-77				707	60	1.5	750		
C22-80-77			2.47	714	80	1.1	750		
C22-80-47				525	80	1.1	750		
S16-45-77	Square		1.30	707	45	2.3	750	4.0	
S16-45-74				707	45	2.3	495		
S16-45-47				516	45	2.3	750		
S16-80-77				707	80	1.3	750		
S22-45-77			2.53	714	45	2.3	750		
S22-45-47				525	45	2.3	750		

As observed in Table 1, two levels of longitudinal reinforcement ratio and two levels of vertical spacing, hence lateral reinforcement ratio were used in both circular and square column specimens. As for yield strength of reinforcements, two levels of SD400 and SD700 were employed in such specimens. Tensile test has been carried out for the reinforcements used in the current study. While yield strengths of SD400 reinforcements are directly achieved from stress-strain relationships, those of SD700 reinforcements are not clearly obtained from the relationships. Thus, 0.2 percent offset method is used to estimate the yield strengths of SD700 reinforcements, as suggested by KCI [15].

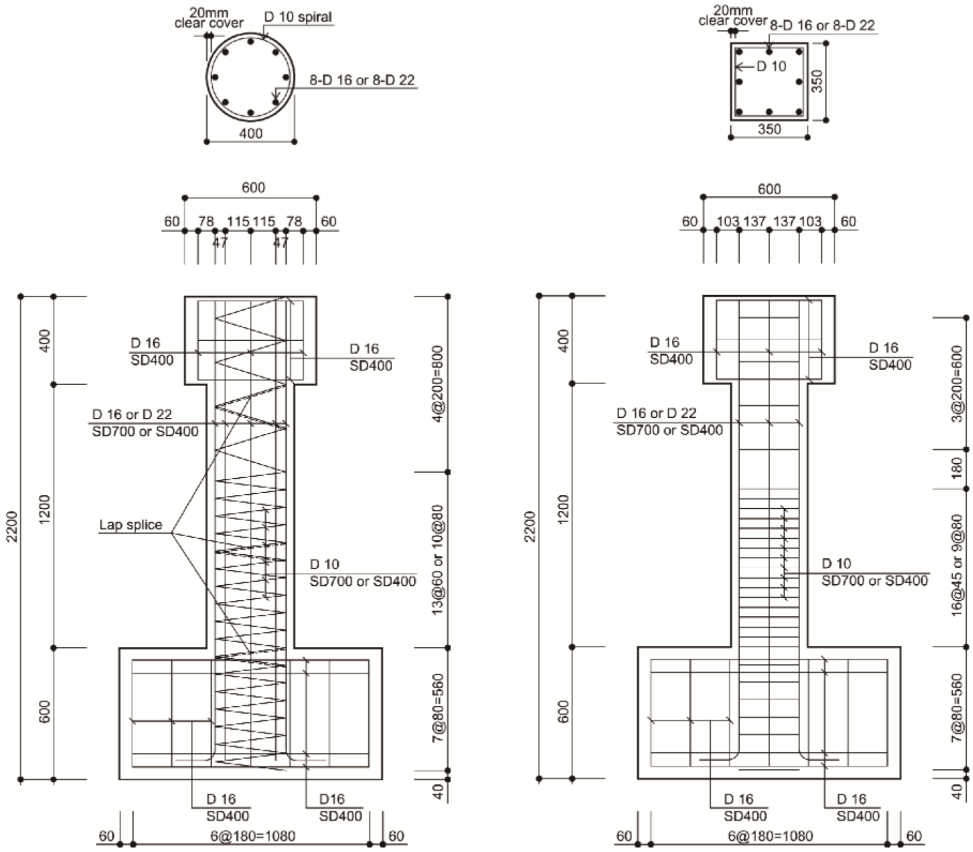

(a) Circular column specimen (b) Square column specimen

Fig. 1 – Dimensions and reinforcement details of column specimens

2.2 Test setup

Each column specimen was tested under a constant axial compression along with increasing lateral deformation reversals. Two hydraulic jacks with a capacity of 2,000 kN were used to apply the constant compressive axial force during the test. A hydraulic actuator with a load capacity of 500 kN was employed to apply the lateral load. Fig. 2 illustrates a test setup. Lateral load was applied by increasing drift ratio in terms of using displacement control. Lateral load reversals consisted of two cycles at each drift ratio, and graphical representation of loading cycles is shown in Fig. 3.

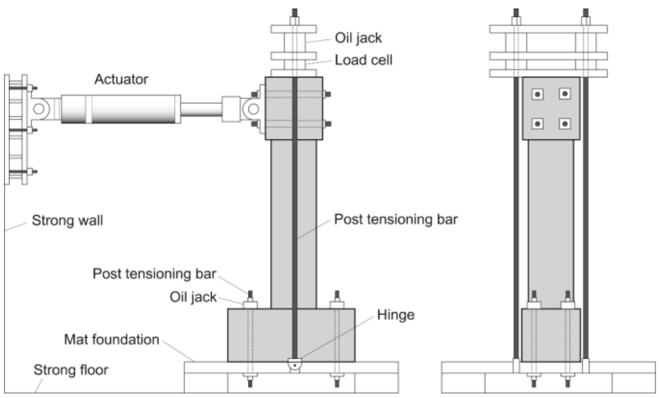

Fig. 2 – Test setup

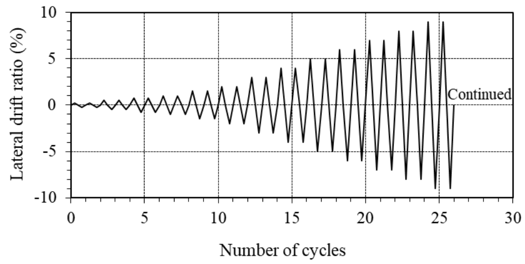

Fig. 3 – Loading cycles

3. Results and discussions

3.1 Crack observation

For specimens C16-80-74, C16-80-47 and S16-45-47, sliding between footing of specimen and mat foundation was occurred, although it was controlled. In addition, S16-45-77 also suffered from a minor sliding. Sliding during test is sometimes difficult to avoid in laboratory testing. Thus, experimental results of the above four specimens were excluded in the following discussion.

First flexural crack perpendicular to column axis was formed at the construction joint between column and footing in all specimens. Then a number of cracks were occurred with increasing load. After yielding of longitudinal reinforcements, cover concrete spalled and crushing of concrete occurred in plastic hinge region as the load increased. All of specimens except for S22-45-77 and S22-45-47 failed in a fracture of longitudinal reinforcement. Whereas specimen S22-45-47 failed in core concrete crushing, specimen S22-45-77 did not fail and test was terminated due to a lack of actuator capacity. Representative failure pattern of circular and square column specimens is displayed in Fig. 4, and type of failure and maximum drift ratio are summarized in Table 2.

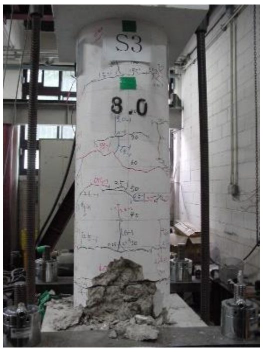

(a) C16-60-77

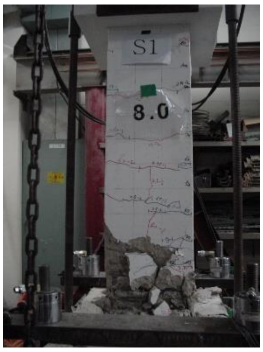

(b) S16-45-74

Fig. 4 – Representative failure pattern of column specimens

Table 2 – Observed type of failure and corresponding maximum drift ratio

Circular columns			**Square columns**		
Specimen	**Observed failure**	**Maximum drift ratio (%)**	**Specimen**	**Obseved failure**	**Maximum drift ratio (%)**
C16-80-77	Fracture	7.0	S16-45-77	Minor sliding	-
C16-80-74	Sliding	-	S16-45-74	Fracture	8.0
C16-80-47	Sliding	-	S16-45-47	Sliding	-
C16-60-77	Fracture	8.0	S16-80-77	Fracture	7.0
C22-80-77	Fracture	8.0	S22-45-77	No failure	9.0
C22-80-47	Fracture	8.0	S22-45-47	Concrete crushing	9.0

3.2 Lateral force-displacement hysteretic response

Figs. 5 and 6 show lateral force-displacement hysteretic response for circular and square column specimens, respectively. Dotted horizontal line represent theoretical lateral force corresponding to maximum moment strength by KCI [15] and ACI 318-14 [12]. Except for those excluded specimens, a very gradual decrease in lateral force is in general observed as displacement increases and thus overall stable response is achieved.

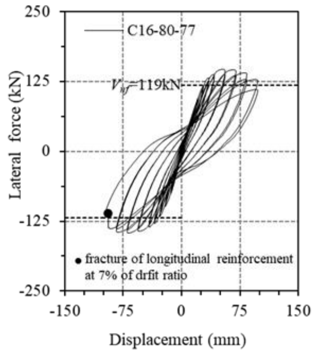

(a) C16-80-77

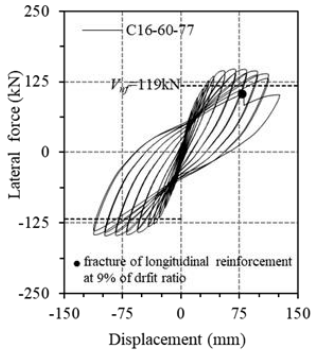

(b) C16-60-77

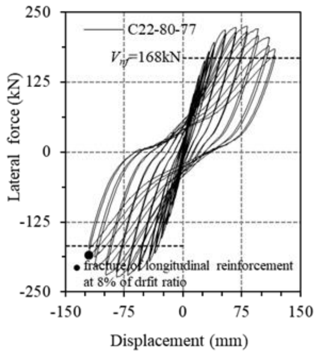

(c) C22-80-77

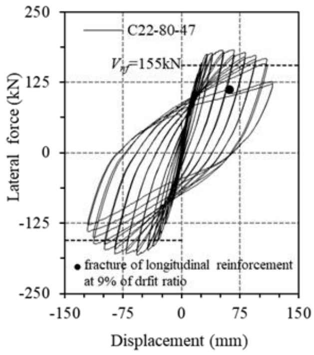

(d) C22-80-47

Fig. 5 – Hysteretic response of circular column specimens

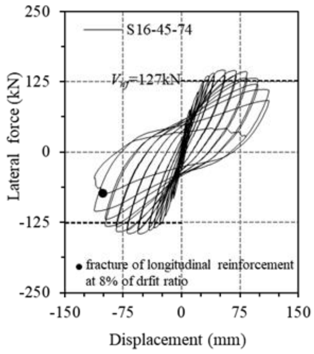

(a) S16-45-74

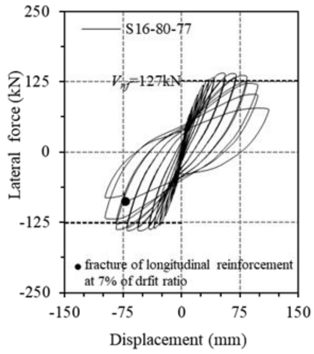

(b) S16-80-77

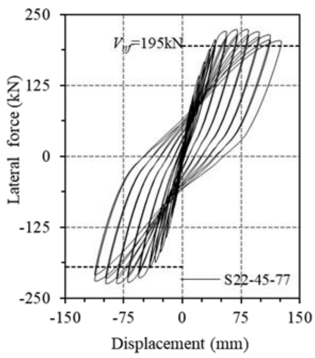

(c) S22-45-77

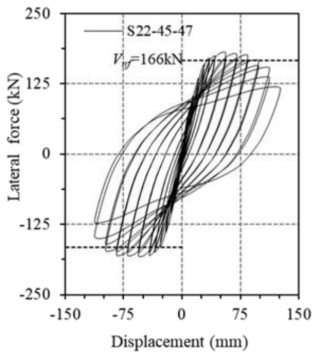

(d) S22-45-47

Fig. 6 – Hysteretic response of square column specimens

As observed in Figs. 5 and 6, specimens with SD700 in both longitudinal and lateral reinforcements show that lateral forces are larger than the code-specified theoretical lateral strength in overall inelastic range. Specimens with SD400 and SD700 of longitudinal and lateral reinforcement respectively show a similar behavior, but strength margin is somewhat reduced. A margin between experimental and theoretical strength is more pronounced in circular column specimens than square column specimens. In addition, the margin is more obvious in specimens with relatively higher longitudinal reinforcement ratio. Although specimens with SD700 of longitudinal reinforcement show higher lateral force carrying capacity and stiffness than those with SD400 of longitudinal reinforcement, a minor pinching is observed in the former specimens, particularly in specimens with higher longitudinal reinforcement ratio. Subsequently, the latter specimens seem to behave in somewhat more ductile manner than the former specimens in terms of slightly better energy dissipation capacity. This behavior is further discussed in the following cumulative energy dissipation capacity.

Meanwhile, it may be somewhat difficult to discuss directly with regard to the effect of SD700 lateral reinforcement on hysteretic response due to those excluded specimens. However, as observed in specimens of S16-45-74 and S16-80-77, high yield strength of lateral reinforcement does not seem to provide a favorable influence on the response. Instead, vertical spacing of the lateral reinforcement seems to play an important role on the response. This can be further supported by comparison between C16-80-77 and C16-60-77. More pronounced ductile behavior is observed in the response of C16-60-77. It is likely to be obvious when a difference in vertical spacing becomes larger.

3.3 Maximum lateral strength

Maximum lateral forces obtained from experiment are compared with those calculated by KCI [15] and ACI 318-14 [12]. Regardless of the symmetric cross section, experimental results in push and pull directions are not identical. This may be due to some asymmetric features that are not uncommon in laboratory testing. Thus, experimental results are averaged in the two direction and summarized in Table 3.

Table 3 – Theoretical and observed maximum lateral strength

Specimen	Theoretical lateral strength (KCI [15], ACI 318-14 [12]), V_{nf} (kN)	Experimental result							
		Push			Pull			Average V_{ave} $\frac{V_{max1}+V_{max2}}{2}$ (kN)	$\frac{V_{ave}}{V_{nf}}$
		V_{max1} (kN)	$\frac{V_{max1}}{V_{nf}}$	Drift ratio (%)	V_{max2} (kN)	$\frac{V_{max2}}{V_{nf}}$	Drift ratio (%)		
C16-80-77	119	151	1.27	3.8	143	1.21	4.9	147	1.24
C16-60-77	119	161	1.36	4.8	134	1.13	6.9	148	1.24
C22-80-77	168	235	1.40	5.8	214	1.28	6.0	225	1.34
C22-80-47	155	191	1.23	4.8	174	1.12	4.0	183	1.18
S16-45-74	127	148	1.17	3.9	142	1.12	3.8	145	1.14
S16-80-77	127	146	1.15	3.7	135	1.07	3.9	141	1.11
S22-45-77	195	223	1.15	5.9	225	1.16	6.9	224	1.15
S22-45-47	166	181	1.09	3.9	182	1.10	3.9	182	1.10

As observed in Table 3, experimental results are in general higher than code-specified theoretical predictions. Whereas the factor of margin is in general pronounced in circular column specimens, it is marginal in square column specimens. Experimental maximum lateral force exhibits 34% and 15% greater than code-specified lateral strength for specimens C22-80-77 and S22-45-77, respectively. In addition, experimental maximum lateral force shows 18% and 10% higher than code-specified lateral strength for specimens C22-80-47 and S22-45-47, respectively. These experimental results indicate that the maximum lateral force of specimen with SD700 longitudinal reinforcement is 23% higher than that of specimen with SD400 longitudinal reinforcement in both circular and square columns. This suggests that there is certainly a favorable effect of SD700 high strength reinforcement on the maximum lateral force carrying capacity.

As for specimens of C16-80-77 and S16-45-74, experimental maximum lateral force exhibits 22% and 14% higher than code-specified lateral strength, respectively. This points out that the factor of margin is slightly higher when longitudinal reinforcement ratio is relatively higher in case of the specimens with SD700 of longitudinal reinforcement. In addition, the margin is more pronounced in circular columns than square columns. This implies that circular cross section columns are likely to be more effective in resisting lateral force than square cross section members even if both have an identical flexural stiffness. Meanwhile, investigation on the vertical spacing of lateral reinforcement reveals that the spacing has little effect on the maximum lateral force carrying capacity, regardless of both cross section and type of lateral reinforcement.

3.4 Displacement ductility

While a reinforced concrete bridge column as a primary member require enough strength to maintain a functionality, the column also needs to have sufficient ductility to prevent a collapse. Ductility represents a deformation capacity of the member and is a measure of the global response of the member to the applied displacement. Ductility can be expressed as a ratio of ultimate displacement divided by yield displacement. Hence, definition of yield and ultimate limit states is of great importance in evaluating the ductility. A globally accepted definition does not exist even though many studies have been carried out aiming at quantifying the limit states for the member [17, 18]. Thus, the most commonly used definition is adopted in the present study. Yield displacement is defined as the point obtained by extrapolating a straight line from the origin through 75% of the maximum lateral force to meet the horizontal line passing through the maximum lateral force. Ultimate displacement is defined as a displacement when 15% reduction of the maximum lateral force occurs. Displacement ductility obtained from experimental results is compared with code-specified ductility. Ductility demand-based seismic design approach in KRTA [14] is used to evaluate the code-specified ductility.

Table 4 – Comparison of displacement ductility

Specimen	**Experimental result**							**Displacement ductility by KRTA [14]**	**Margin of Safety**
	Yield displacement (mm)			**Ultimate displacement (mm)**			**Displacement ductility**		
	Push	**Pull**	**Ave.**	**Push**	**Pull**	**Ave.**	**Ave.**		
C16-80-77	24	25	24.5	98	94	96	4.0	4.0	1.00
C16-60-77	18	29	23.5	119	112	116	5.0	5.0	1.00
C22-80-77	22	29	25.5	117	119	118	4.6	3.6	1.28
C22-80-47	18	27	22.5	118	116	117	5.2	4.6	1.13
S16-45-74	22	22	22.0	104	103	104	4.9	3.2	1.53
S16-80-77	21	23	22.0	99	97	98	4.5	2.8	1.61
S22-45-77	28	28	28.0	126	112	119	4.3	3.9	1.10
S22-45-47	24	23	23.5	114	110	112	4.8	5.1	0.94

Comparison between experiment and code-specified displacement ductility for circular and square column specimens is made and summarized in Table 4. Experimental displacement ductility values are averaged in push and pull directions due to asymmetric feature of testing, as mentioned previously. It is noteworthy that experimental maximum displacement is assumed as an ultimate displacement when 15% reduction of maximum lateral force does not occur in lateral force-displacement envelope curve of a specimen.

As observed in Table 4, experimental ductility values are in general greater than code-specified values. Although experimental ductility values for specimens of C16-80-77, C16-60-77 and S22-45-77 are almost same as code-specified ones, the former values are eventually expected to be greater than the latter values, particularly for circular column specimens. This can be attributed to the fact that the former values are calculated using experimental maximum displacement since 15% reduction did not occur in such members. Subsequently, margin of safety for specimens C16-80-77 and C16-60-77 is likely to be greater than that of 1.28 and 1.13 estimated for specimens C22-80-77 and C22-80-47, respectively. This can be supported by evaluation on the margin of safety for square column specimens. While the margin of safety is 1.53 and 1.61 for specimens S16-45-74 and S16-80-77, respectively, that is reduced for specimens S22-45-77 and S22-45-47 where higher longitudinal reinforcement ratio is employed. This observation suggests that experimental ductility value is influenced by both yield strength and ratio of longitudinal reinforcement. In turn, the higher yield strength and ratio of longitudinal reinforcement, the lower the displacement ductility. It is thus postulated that deformation capacity hence ductility is not likely proportional to yield strength of reinforcement, unlike lateral load carrying capacity.

Meanwhile, experimental result reveals that ductility values of circular column specimens are overall greater than those of square columns. In addition, those values increase as vertical spacing reduces, and an increment of the values is more pronounced in specimens with spiral confining hoops as expected.

3.5 Cumulative energy

Cumulative energy dissipation capacity is evaluated at each cycle in terms of integrating areas bounded by hysteresis loops for both specimens and is illustrated graphically in Fig. 7. In general, cumulative energy dissipation is similar up to the 14th cycle for both specimens as shown in Fig. 7. However, beyond the cycle, a discrepancy is seen in between specimens as the members undergo increased inelastic displacement. Abrupt increase occurs in specimens C22-80-47 and S22-45-47, while relatively asymptotic increase is observed in other specimens. This tendency correlates well with the results of displacement ductility evaluation. In turn, cumulative energy dissipation capacity also does not seem to be proportional with yield strength of longitudinal reinforcement.

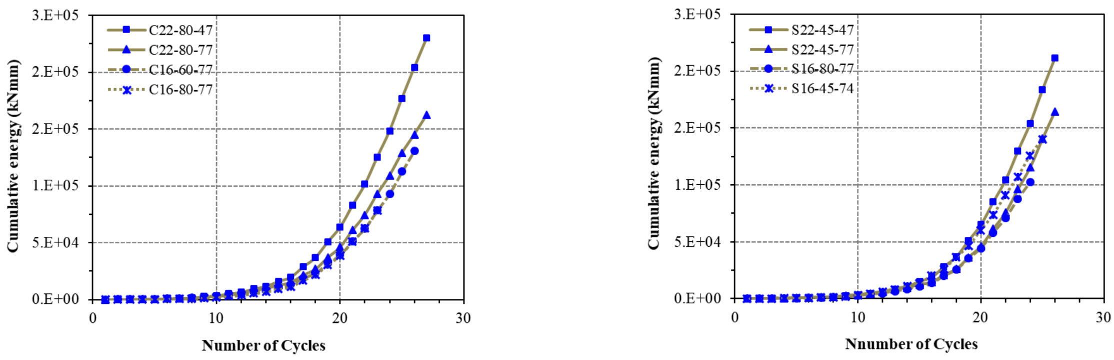

(a) Circular column specimens (b) Square column specimens

Fig. 7 – Comparison of cumulative energy

Also observed in Fig. 7 is that circular column specimens exhibit overall higher cumulative energy dissipation capacity than square members. In addition, specimens with relatively higher longitudinal reinforcement ratio show a better energy dissipation capacity than those with lower longitudinal reinforcement ratio. Moreover, higher cumulative energy dissipation capacity is achieved in specimens with smaller vertical spacing of lateral reinforcement. It is thus worth noting that longitudinal reinforcement ratio and vertical spacing of lateral reinforcement are salient features for energy dissipation.

4. Conclusions

Seismic performance evaluation has been carried out for reinforced concrete bridge columns employing normal (SD400) and high (SD700) yield strength of reinforcement. For this purpose, a total of 12 columns, i.e., 6 circular and 6 square cross section specimens have been tested under simulated lateral load reversals. Salient parameters considered in the present study are yield strength of longitudinal and lateral reinforcement, longitudinal reinforcement ratio, and vertical spacing of lateral reinforcement.

Lateral force-displacement hysteretic response reveals that lateral forces are in general well above the code-specified lateral strength in overall displacement range. A difference between the two lateral forces is more marginal in specimens with SD700 of longitudinal reinforcement than specimens with SD400 of longitudinal reinforcement, particularly for circular columns. Although the above both specimens exhibit stable behavior, the latter specimens show somewhat more ductile response than the former specimens. This tendency is particularly pronounced in specimens with relatively higher longitudinal reinforcement ratio.

Maximum lateral strength indicates that experimental results are in general higher than code-specified theoretical predictions. In particular, maximum lateral force of specimen with SD700 longitudinal reinforcement is 23% higher than that of specimen with SD400 longitudinal reinforcement in both circular and square columns.

Comparison between experimental and code-specified displacement ductility implies that ductility value is affected by both yield strength and ratio of longitudinal reinforcement. The value is rather reduced as yield strength and ratio of longitudinal reinforcement are increased. This is further supported in terms of observation on cumulative energy dissipation capacity. Consequently, deformation capacity does not seem to be proportional with yield strength of longitudinal reinforcement.

In summary, use of high yield strength reinforcement in reinforced concrete columns has apparently a favorable effect on maximum lateral force carrying capacity throughout the displacement range, leading stable hysteretic response. However, the current evaluation on the deformation capacity indicates that ductility and energy dissipation is less marginal in specimens with high yield strength reinforcement in comparison with the maximum lateral force carrying capacity. It is thus concluded that additional experimental study is required to clarify further the deformation capacity of reinforced concrete columns with high yield strength of reinforcement.

5. Acknowledgements

This work was supported by the National Research Foundation of Korea (NRF) grant funded by the Korea government (MSIT: Ministry of Science and ICT) (No. NRF-2018R1A2B6005716).

6. Copyrights

7. References

[1] Ansley MH (2002): Investigation into the structural performance of MMFX reinforcing bars. *Structures Research Project Report*. Florida Department of Transportation; USA.

[2] Watanabe F and Nishiyama M (2003): Controlled yield sequence of reinforcement in concrete members. High Performance Materials in Bridges. *Proceedings of the International Conference*, Hawaii, 87-96.

[3] Hassan TK, Seliem HM, Dwairi H, Rizkalla SH, Zia P (2008): Shear behavior of large concrete beams reinforced with high-strength steel. *ACI Structural Journal*, **105**(2), 173-179.

[4] Mast RF, Dawood M, Rizkalla SH, Zia P (2008): Flexural strength design of concrete beams reinforced with high-strength steel bars. *ACI Structural Journal*, **105**(4), 570-577.

[5] Sumpter MS, Rizkalla SH, Zia P (2009): Behavior of high-performance steel as shear reinforcement for concrete beams. ACI Structural Journal, **106**(2), 171-177.

[6] Lee J-Y, Choi IJ, Kang JE (2010): Evaluation of the maximum yield strength of steel stirrups and shear behavior of RC beams. *Journal of the Korea Concrete Institute*, **22**(5), 711-718.

[7] Hwang H-J, Park H-G, Choi W-S, Lan C, Kim J-K (2011): Seismic performance of beam-column connections for special moment frame using 600MPa flexural reinforcement. *Journal of the Korea Concrete Institute*, **23**(5):591-601.

[8] Lee J-Y, Choi S-H, Lee DH (2018): Practicability of large-scale reinforced concrete beams using Grade 80 stirrups. *ACI Structural Journal*, **15**(1), 269-280.

[9] Yoon S-K, Lee S-C, Lee DH, Lee J-Y (2014): Failure modes of RC beams with high strength reinforcement. *Journal of the Korea Concrete Institute*, **26**(2), 143-150.

[10] Lee J-Y, Lee DH, Lee J-E, Choi S-H (2015): Shear behavior and diagonal crack width for reinforced concrete beams with high-strength shear reinforcement. *ACI Structural Journal*, **112**(3), 323-333.

[11] Lee J-Y, Choi S-H, Lee DH (2016): Structural behavior of reinforced concrete beams with high yield strength stirrups. *Magazine of Concrete Research*, **68**(23), 1187-1199.

[12] ACI Committee 318 (2015): *Building code requirements for structural concrete (ACI 318M-14) and commentary (ACI 318RM-14)*. American Concrete Institute.

[13] BS EN 1992-1-1 (2004): *Eurocode 2: Design of concrete structures, part 1-1 general rules and rules for buildings*. European Committee for Standardization (CEN).

[14] KRTA (2015): *Design code for highway bridges (limit state design)*. Korea Road and Transportation Association, Korea.

[15] KCI (2017): *KCI model code*. Korea Concrete Institute.

[16] KS D 3504 (2016): *Steel bars for concrete reinforcement*. Korea Agency for Technology and standards.

[17] Lee DH, Park J, Lee K, Kim BH (2011): Nonlinear seismic assessment for the post-repair response of RC bridge piers. *Composites Part B: Engineering*, **42**(5), 1318-1329.

[18] Jeon J-S, Shafieezadeh A, Lee DH, Choi E, DesRoches R (2015): Damage assessment of older highway bridges subjected to three-dimensional ground motions: characterization of shear-axial force interaction on seismic fragilities. *Engineering Structures*, **87**, 47-57.

